

Rare decays $\bar{B} \rightarrow X_{s(d)}\gamma$ at the NLO

H. M. Asatrian, H. H. Asatryan, A. Hovhannisyan

Yerevan Physics Institute, 2 Alikhanyan Br., 375036, Yerevan, Armenia

Abstract

We present an independent calculation of $\mathcal{O}(\alpha_s)$ matrix elements of the QCD penguin operators for the decays $\bar{B} \rightarrow X_{s(d)}\gamma$. The Mellin-Barnes representation technique is applied for the systematic numerical evaluation of involved two-loop diagrams. The numerical effect of the calculated contributions is confirmed to be of order of 1%. We also present an updated numerical analysis for $\bar{B} \rightarrow X_{s(d)}\gamma$ decay rates.

1 Introduction

The rare B decays play a special role in the phenomenology of weak decays. They are loop-induced in the standard model (SM) and thus are strongly affected by many contributions from the new sources of flavor violation in various extensions of the SM. The inclusive rare transitions are of particular interest as they are well approximated by the underlying partonic transitions. The corrections to this perturbative picture are calculable within the framework of Heavy Quark Effective Theory (HQET).

Among the rare B-decays the inclusive $\bar{B} \rightarrow X_s \gamma$ transition is the most interesting one. Since the first observation of the decay by the CLEO [1] new measurements have been reported by ALEPH, BELLE and BABAR [2]- [5]. The CLEO still has the best determination [6]:

$$\mathcal{B}(\bar{B} \rightarrow X_s \gamma) = (3.21 \pm 0.43 \pm 0.27_{-0.10}^{+0.18}) \times 10^{-4}. \quad (1.1)$$

while the current world average is [7]

$$\mathcal{B}(\bar{B} \rightarrow X_s \gamma) = (3.40 \pm 0.39) \times 10^{-4}. \quad (1.2)$$

The CKM-suppressed counterpart $\bar{B} \rightarrow X_d \gamma$ decay is also promising. However, no experimental observations of the $b \rightarrow d \gamma$ mediated transitions have been made so far. The upper experimental limits for the exclusive decays $B \rightarrow \rho^{\pm(0)} \gamma, B \rightarrow \omega \gamma$ [8] are higher than the corresponding theoretical predictions roughly by a factor of 2.

As for the theoretical side, calculation of the NLO perturbative QCD corrections for the decay $\bar{B} \rightarrow X_s \gamma$ has been completed in [9]-[18]. These corrections lead to dramatic reduction of the renormalization scale dependence of the leading order (LO) results bringing the uncertainty in theoretical predictions for the decay rate to the level of 10% and opening the door for a rigorous comparison with experimental data. The leading order long distance corrections within the framework of HQET have been computed in [19]-[21]. Also the leading electroweak corrections are known [22]. The comparison of the current theoretical predictions with the available experimental data already presents strong constraints on the extensions of the SM (see e.g. [23] for a recent analysis). These analyses have been extended to the case of $\bar{B} \rightarrow X_d \gamma$ decay in [24]-[26].

Only about two years ago the last missing ingredients of the full NLO result- $\mathcal{O}(\alpha_s)$ matrix elements of the QCD-penguin operators, have been calculated in [18]. The calculation is complicated due to large number of contributing non-trivial two-loop diagrams, so a verifying re-calculation is desirable. In this paper we present an independent computation of these matrix elements. We apply the Mellin-Barnes representation technique for the systematic numerical calculation of the involved two-loop diagrams. This is in contrast to the method of [18] where the results are expressed in terms of a few integrals to be evaluated numerically. We confirm their numerical results and extend the analysis to the case of $\bar{B} \rightarrow X_d \gamma$ decay (see also [28] for a very recent similar analysis).

The paper is organized as follows. In Section 2 we present the effective Hamiltonians for the decays $\bar{B} \rightarrow X_{s(d)} \gamma$ and collect the final results for the matrix elements of the dimension-6 operators. Section 3 is devoted to the details of our calculation method. In Section 4 we give

an update of numerical predictions for the branching fractions for $\bar{B} \rightarrow X_{s(d)}\gamma$. Some of the useful formulae are collected in appendices.

2 The decay rates for $\bar{B} \rightarrow X_{s(d)}\gamma$

The effective Hamiltonian for the decay $b \rightarrow s\gamma$ (and the associated bremsstrahlung process $b \rightarrow s\gamma g$) reads

$$\mathcal{H}_{eff}(b \rightarrow s\gamma) = -\frac{4G_F}{\sqrt{2}} \left(\lambda_t^{(s)} \sum_{i=1}^8 C_i O_i - \lambda_u^{(s)} \sum_{i=1}^2 C_i (O_i^u - O_i) \right) \quad (2.1)$$

where the CKM factors are given by

$$\lambda_t^{(s)} \equiv V_{ts}^* V_{tb} = -A\lambda^2 \left(1 - \frac{A^2\lambda^4}{2} \right) \left(1 - \frac{\lambda^2}{2} + \lambda^2(\rho - i\eta) \right), \quad \lambda_u^{(s)} \equiv V_{us}^* V_{ub} = A\lambda^4(\rho - i\eta). \quad (2.2)$$

The Wilson coefficients $C(\mu)$ are known to $\mathcal{O}(\alpha_s)$ precision. We refer to [16] and references therein for the explicit formulae. The dimension six effective operators can be chosen as

$$\begin{aligned} O_1^u &= (\bar{s}_L \gamma_\mu T^a u_L)(\bar{u}_L \gamma^\mu T^a b_L), & O_2^u &= (\bar{s}_L \gamma_\mu u_L)(\bar{u}_L \gamma^\mu b_L), \\ O_1 &= (\bar{s}_L \gamma_\mu T^a c_L)(\bar{c}_L \gamma^\mu T^a b_L), & O_2 &= (\bar{s}_L \gamma_\mu c_L)(\bar{c}_L \gamma^\mu b_L), \\ O_3 &= (\bar{s}_L \gamma_\mu b_L) \sum_q (\bar{q} \gamma^\mu q), & O_4 &= (\bar{s}_L \gamma_\mu T^a b_L) \sum_q (\bar{q} \gamma^\mu T^a q), \\ O_5 &= (\bar{s}_L \gamma_\mu \gamma_\nu \gamma_\rho b_L) \sum_q (\bar{q} \gamma^\mu \gamma^\nu \gamma^\rho q), & O_6 &= (\bar{s}_L \gamma_\mu \gamma_\nu \gamma_\rho T^a b_L) \sum_q (\bar{q} \gamma^\mu \gamma^\nu \gamma^\rho T^a q), \\ O_7 &= \frac{e}{16\pi^2} m_b (\bar{s}_L \sigma^{\mu\nu} b_R) F_{\mu\nu}, & O_8 &= \frac{e}{16\pi^2} m_b (\bar{s}_L \sigma^{\mu\nu} b_R) F_{\mu\nu}, \end{aligned} \quad (2.3)$$

The corresponding formulae for the decays $b \rightarrow d\gamma(g)$ can be obtained from Eqs.(2.1),(2.3) with the obvious replacement $s \rightarrow d$. The relevant CKM factors read

$$\lambda_t^{(d)} \equiv V_{td}^* V_{tb} = A\lambda^3 \left(1 - \frac{A^2\lambda^4}{2} \right) (1 - \bar{\rho} + i\bar{\eta}), \quad \lambda_u^{(d)} \equiv V_{ud}^* V_{ub} = A\lambda^3(\bar{\rho} - i\bar{\eta}). \quad (2.4)$$

Taking into account that λ is small ($\lambda \simeq 0.22$) one can safely neglect the terms proportional to $\lambda_u^{(s)}$ in the case of $b \rightarrow s\gamma$. In the case of $b \rightarrow d\gamma$ however these terms are important in particular being responsible for the generation of a large CP-asymmetry. We will keep those terms both in analytical and numerical formulae.

The decay widths for the partonic transitions can be expressed as

$$\begin{aligned} \Gamma[b \rightarrow s(d)\gamma]^{E_\gamma > E_0 \equiv (1-\delta)m_b/2} &= \\ &= \frac{G_F^2 \alpha_{em}}{32\pi^4} |\lambda_t^{s(d)}|^2 m_{b,pole}^3 m_{b,\overline{MS}}^2(m_b) \left(|D^{s(d)} + \epsilon_{ew}|^2 + A^{s(d)} \right), \end{aligned} \quad (2.5)$$

where we have separated the virtual and bremsstrahlung corrections. At the NLO we have

$$\begin{aligned}
D^{s(d)} &= C_7^{(0)eff}(\mu_b) + \frac{\alpha_s(\mu_b)}{4\pi} \left(C_7^{(1)eff}(\mu_b) + \sum_{i=1}^8 C_i^{(0)eff}(\mu_b) \left[r_i + \gamma_{i7}^{(0)eff} \ln \frac{m_b}{\mu_b} \right] \right) \\
&- \frac{\lambda_u^{s(d)}}{\lambda_t^{s(d)}} \frac{\alpha_s}{4\pi} \sum_{i,j=1}^2 C_i^{(0)eff}(\mu_b) [r_i^u - r_i], \tag{2.6}
\end{aligned}$$

$$\begin{aligned}
A^{s(d)} &= \frac{\alpha_s}{\pi} \left\{ \sum_{i,j=1}^8 C_i C_j f_{ij}^{cc} - 2\text{Re} \left[\frac{\lambda_u^{s(d)} \lambda_t^{s(d)}}{|\lambda_t^{s(d)}|^2} \sum_{i=1}^8 \sum_{j=1}^2 C_i C_j (f_{ij}^{uc} - f_{ij}^{cc}) \right] \right. \\
&+ \left. \left| \frac{\lambda_u^{s(d)}}{\lambda_t^{s(d)}} \right|^2 \sum_{i,j=1}^2 C_i C_j [f_{ij}^{uu} + f_{ij}^{cc} - 2\text{Re} f_{ij}^{uc}] \right\}. \tag{2.7}
\end{aligned}$$

The formulae for the bremsstrahlung coefficients f_{ij} are presented in Appendix B. ϵ_{ew} represents the leading electroweak correction that can be extracted from [22].

The quantities r_i are given by

$$\begin{aligned}
r_1 &= -\frac{1}{6}r_2, & r_2 &= -\frac{1666}{243} + 2(a(z) + b(z)) - \frac{80}{81}i\pi, \\
r_3 &= 10.059 + \frac{28}{81}i\pi, & r_4 &= -1.017 - \frac{110}{243}i\pi + 2b(z), \\
r_5 &= 185.841 + \frac{448}{81}i\pi, & r_6 &= -8.148 - \frac{2480}{243}i\pi + 12a(z) + 20b(z), \\
r_7 &= -\frac{10}{3} - \frac{8\pi^2}{9}, & r_8 &= \frac{44}{9} - \frac{8}{27}\pi^2 + \frac{8}{9}i\pi,
\end{aligned} \tag{2.8}$$

and $r_i^u = \lim_{z \rightarrow 0} r_i (i = 1, 2)$. We will present the calculation of the matrix elements r_3, \dots, r_6 in some detail in Section 3. In Eq. (2.8) we have used the functions $a(z), b(z)$ defined in [18] to encode z -dependent part of the matrix elements of the current-current operators O_1 and O_2 :

$$\begin{aligned}
a(z) &= \frac{16}{9} \left\{ \left(\frac{5}{2} - \frac{1}{3}\pi^2 - 3\zeta(3) + \left(\frac{5}{2} - \frac{3}{4}\pi^2 \right) L + \frac{1}{4}L^2 + \frac{1}{12}L^3 \right) z \right. \\
&+ \left(\frac{7}{4} + \frac{2}{3}\pi^2 - \frac{1}{2}\pi^2 L - \frac{1}{4}L^2 + \frac{1}{12}L^3 \right) z^2 + \left(-\frac{7}{6} - \frac{1}{4}\pi^2 + 2L - \frac{3}{4}L^2 \right) z^3 \\
&+ \left(\frac{457}{216} - \frac{5}{18}\pi^2 - \frac{1}{72}L - \frac{5}{6}L^2 \right) z^4 + \left(\frac{35101}{8640} - \frac{35}{72}\pi^2 - \frac{185}{144}L - \frac{35}{24}L^2 \right) z^5 \\
&+ \left(\frac{67801}{8000} - \frac{21}{20}\pi^2 - \frac{3303}{800}L - \frac{63}{20}L^2 \right) z^6 + i\pi \left[\left(2 - \frac{1}{6}\pi^2 + \frac{1}{2}L + \frac{1}{2}L^2 \right) z \right. \\
&+ \left. \left(\frac{1}{2} - \frac{1}{6}\pi^2 - L + \frac{1}{2}L^2 \right) z^2 + z^3 + \frac{5}{9}z^4 + \frac{49}{72}z^5 + \frac{231}{200}z^6 \right] \left. \right\} + O(z^7), \tag{2.9}
\end{aligned}$$

$$\begin{aligned}
b(z) &= -\frac{8}{9} \left\{ \left(-3 + \frac{1}{6}\pi^2 - L \right) z - \frac{2}{3}\pi^2 z^{3/2} + \left(\frac{1}{2} + \pi^2 - 2L - \frac{1}{2}L^2 \right) z^2 \right. \\
&+ \left(-\frac{25}{12} - \frac{1}{9}\pi^2 - \frac{19}{18}L + 2L^2 \right) z^3 + \left(-\frac{1376}{225} + \frac{137}{30}L + 2L^2 + \frac{2}{3}\pi^2 \right) z^4 \\
&+ \left(-\frac{131317}{11760} + \frac{887}{84}L + 5L^2 + \frac{5}{3}\pi^2 \right) z^5 + \left(-\frac{2807617}{97200} + \frac{16597}{540}L + 14L^2 + \frac{14}{3}\pi^2 \right) z^6 \\
&+ i\pi \left[-z + (1 - 2L) z^2 + \left(-\frac{10}{9} + \frac{4}{3}L \right) z^3 + z^4 + \frac{2}{3}z^5 + \frac{7}{9}z^6 \right] \left. \right\} + O(z^7), \tag{2.10}
\end{aligned}$$

where $L = \ln z$ ¹.

Following [23] we use the following formula for the branching ratios:

$$\mathcal{B}(\bar{B} \rightarrow X_{s(d)\gamma}) = \mathcal{B}(B \rightarrow X_c e \bar{\nu})^{exp} \frac{\Gamma(\bar{B} \rightarrow X_{s(d)\gamma})}{C |V_{cb}/V_{ub}|^2 \Gamma(B \rightarrow X_u e \bar{\nu})} \quad (2.11)$$

The essential reason for introducing (2.11) is that the factor

$$C = \left| \frac{V_{ub}}{V_{cb}} \right|^2 \frac{\Gamma(B \rightarrow X_c e \bar{\nu})}{\Gamma(B \rightarrow X_u e \bar{\nu})}$$

can be predicted with relatively small uncertainty using the Υ expansion [29]. We use $C = 0.575 \times (1 \pm 0.03)$ as estimated in [23]. As it follows from Eq. (2.11) $\mathcal{O}(\alpha_s)$ corrections for the inclusive decay $B \rightarrow X_u e \bar{\nu}$ have to be included in our analysis.

When doing the transition to B-meson decay rates in Eq. (2.11) from the corresponding partonic decay rates one has to include the leading $1/m_b^2$ [19] and $1/m_c^2$ corrections [21]. Note that in the case of $\bar{B} \rightarrow X_d \gamma$ additional long-distance contributions due to intermediate u -quark loops can have a sizeable effect. These contributions can not be reliably predicted but the model calculations indicate that they are not very large [30],[31]. In the present paper we will ignore them.

3 Calculation of the virtual $\mathcal{O}(\alpha_s)$ corrections for the operators O_3, \dots, O_6 .

3.1 Organization of the calculation

We start describing the virtual $\mathcal{O}(\alpha_s)$ contributions to the matrix elements of the operators O_3, \dots, O_6 . The relevant Feynman diagrams are depicted in Fig.1. Note that the full set of contributing diagrams is larger, however, the calculation of the other diagrams can be avoided if one uses the gauge invariance of the result. Furthermore, the contributions of some of the diagrams are already included when one uses the effective Wilson coefficient C_7^{eff} instead of C_7 .

Note that for each of the diagrams there are two possible types of operator insertions as illustrated in Fig.2. Apparently for type I insertions only b and s quark loops contribute while all five (u, d, s, c and b) quarks can give non-zero type II contributions. In our calculations we set the masses of the light quarks u, d, s to zero.

Our calculation extends the method described in [17]. While for the light and c quark contributions it is straightforward, for the evaluations of the diagrams with b quark in the loop we use a different tactics to get numerical results. As we think that our method can be useful in other similar calculations we describe it in some detail in subsection 3.2.

¹Originally these functions have been calculated in [17] with precision of $\mathcal{O}(z^3)$ and later extended to include terms up to z^6 in [27]. We have verified these expressions using the method of [17] to include terms $\mathcal{O}(z^4)$, $\mathcal{O}(z^5)$, and $\mathcal{O}(z^6)$.

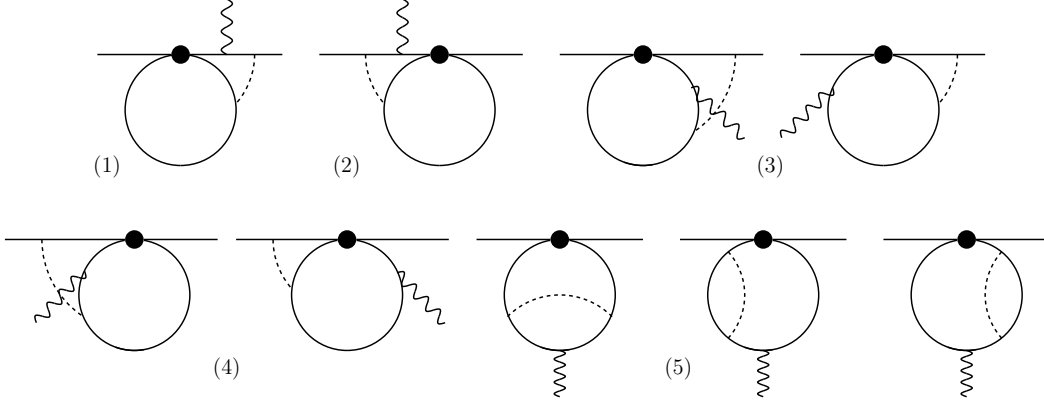


Figure 1: The diagrams contributing to the matrix elements of the operators O_3, \dots, O_6 .

For a better organization of our computation we will use the following decomposition:

$$O_3 = (\bar{s}\gamma_\mu Lb) \sum_q (\bar{q}\gamma^\mu Lq) + (\bar{s}\gamma_\mu Lb) \sum_q (\bar{q}\gamma^\mu Rq) \equiv O_{3L} + O_{3R},$$

$$O_4 = (\bar{s}\gamma_\mu LT^a b) \sum_q (\bar{q}\gamma^\mu LT^a q) + (\bar{s}\gamma_\mu LT^a b) \sum_q (\bar{q}\gamma^\mu RT^a q) \equiv O_{4L} + O_{4R}$$

and similarly for the operators O_5, O_6 .

Following the ref. [17], as a first step in the calculation of the two-loop diagrams in Fig.1 we evaluate the building blocks from Fig.4. We present the full expressions of the one-loop building blocks in Appendix A. As we are going to illustrate the method of our calculation in the next subsection we will give here the expression for the contribution of O_{3L} with b -quark loop to the building block I_β :

$$I_{\beta(3)}^{b(I)}(L) = -\frac{g_s}{4\pi^2} \Gamma(\epsilon) (1-\epsilon) \mu^{2\epsilon} e^{\gamma_E \epsilon} e^{i\pi\epsilon} \int_0^1 \frac{dx [x(1-x)]^{1-\epsilon}}{\Delta^\epsilon} (r_\beta \not{x} - r^2 \gamma_\beta) L \frac{\lambda}{2} \quad (3.1)$$

where

$$\Delta = r^2 - m_q^2/x(1-x) + i\delta. \quad (3.2)$$

3.2 The method of the calculation

We will illustrate our method of calculation on the example of diagram (1) from Fig.1 for the type I insertion of the operator O_{3L} . Using (3.1) and applying the standard technique of the Feynman parameterization for the integration over the second 4-momentum we arrive to ²

$$M(1c) = \frac{eQ_a g_s^2 C_F}{64\pi^4} \Gamma(2\epsilon) \exp^{2i\pi\epsilon} \int dx du dv dy [x(1-x)]^{1-\epsilon} y^{\epsilon-1} (1-v)^\epsilon v \times$$

²The details of the calculation of the same diagram with a charm-quark loop for the operator O_2 are given in [17].

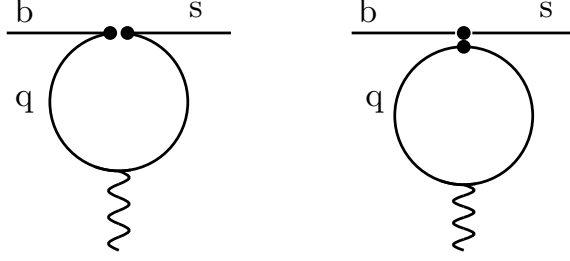


Figure 2: **Two types of operator insertions contributing to $b \rightarrow s(d)\gamma$.**

$$\bar{u}(p') \left[P_1 \frac{\hat{C}}{\hat{C}^{2\epsilon}} + P_2 \frac{1}{\hat{C}^{2\epsilon}} + P_3 \frac{1}{\hat{C}^{1+2\epsilon}} \right] u(p) \quad (3.3)$$

where the integration over the Feynman parameters x, y, u, v is over the interval $[0;1]$ and \hat{C} is given by

$$\hat{C} = m_b^2 v(1-v)u - m_q^2 \frac{(1-v)y}{x(1-x)} + i\delta \quad (3.4)$$

The strategy in [17] (as well as in the similar calculations [32], [33]) is then to use the Mellin-Barnes representation for the integrals in eq. (3.3) which is given by

$$\frac{1}{(k^2 - M^2)^\lambda} = \frac{1}{(k^2)^\lambda} \frac{1}{\Gamma(\lambda)} \frac{1}{2\pi i} \int_\gamma ds (-M^2/k^2)^s \Gamma(-s) \Gamma(\lambda + s) \quad (3.5)$$

where $\lambda > 0$ and the integration path goes parallel to the imaginary axis in the complex s -plane hitting the real axis somewhere between $-\lambda$ and 0 . In [17] the formula (3.5) is applied to the denominators in (3.3) using the identification

$$k^2 \leftrightarrow m_b^2 v(1-v)u ; \quad M^2 \leftrightarrow m_q^2 \frac{(1-v)y}{x(1-x)} \quad (3.6)$$

Then the integrals over the Feynman parameters are expressed in terms of Euler's Γ -functions. To evaluate the integral over the Mellin-Barnes parameter s the integration path is closed in the right s -half-plane. When $m_q^2/m_b^2 < 1/4$ the integral over the half-circle vanishes so using the residue theorem the integral is expressed as the sum over residues in the integration contour. This in turn leads to a natural expansion in the (small) parameter m_q^2/m_b^2 .

This procedure apparently won't work for the case $q = b$. The absence of a small expansion parameter seems to make the described technique unapplicable in this case. However we note that the appearance of the factor $x(1-x)$ ($0 \leq x \leq 1$) in eq. (3.4) plays a role of a suppression factor for the second term and it turns out that the 'opposite' identification

$$M^2 \leftrightarrow m_b^2 v(1-v)u, \quad k^2 \leftrightarrow m_q^2 \frac{(1-v)y}{x(1-x)} \quad (3.7)$$

does a better job in the case $q = b$. Just as in [17] then we first take the integrals over the Feynman parameters which after appropriate substitutions can be brought into the following forms:

$$\int_0^1 dw w^p, \quad \int_0^1 dw w^p (1-w)^q = \frac{\Gamma(p+1)\Gamma(q+1)}{\Gamma(p+q+2)}$$

Then to perform the integration over s we can close the integration path in the right half-plane and use the residue theorem. The relation $x(1-x) \leq 1/4$ guarantees then that the integral over the half-circle vanishes.

So the integrals will be reduced to sums over the residues of Γ function that reside on the real axis (in complex s -plane):

$$s = n, \quad n - \epsilon, \quad n - 2\epsilon \quad (n = 0, 1, 2, \dots), \quad s = m/2 - 2\epsilon, \quad (m = 3, 5, \dots) \quad (3.8)$$

We note again that though there is no real expansion parameter, the terms with higher values of n (or m) are suppressed because of factor $x(1-x)$. So taking into account only first several values of n makes a good numerical approximation of the final result.

It is easy to check the validity of our procedure for the diagram (1) from Fig. 1. as it can be calculated analytically (see formula (5.6) of ref. [18])). Summing over the residues at $n = 0, \dots, 6$ (see Eq.(3.8)) we will get real good approximation for the final result with the precision of 10^{-6} . We didn't observe such a fast convergence for the other diagrams, however the sum over the several first values of n in all of the cases gives a good approximation for the involved integrals. For each of the diagrams we will keep as many poles as it is necessary for getting a precision of at least 10^{-3} .

3.3 Results of the calculation

Using the method described above we are able to calculate the unrenormalized matrix element of the operator O_3 . We find

$$M_3 = \left(\frac{248}{81} \frac{1}{\epsilon} \left(\frac{m_b}{\mu} \right)^{-4\epsilon} + 9.357 + \frac{100}{81} i\pi \right) \times \frac{\alpha_s}{4\pi} \langle s\gamma | O_7 | b \rangle_{tree} \quad (3.9)$$

Looking at the expressions for the building blocks it is easy to see that the contributions from the operators can be expressed in terms of corresponding contributions from O_3 with multiplicative factors that can be extracted from the formulae in Appendix A. The diagrams from Fig. 1.5 that do not contain the building blocks are easy to calculate without any numerical approximations. The results for the unrenormalized matrix elements of the remaining operators are

$$M_4 = \left(-\frac{46}{243\epsilon} \left(\frac{m_b}{\mu} \right)^{-4\epsilon} - 0.899 + 2 b(z) - \frac{146}{243} i\pi \right) \times \frac{\alpha_s}{4\pi} \langle s\gamma | O_7 | b \rangle_{tree}$$

$$M_5 = \left(\frac{5552}{81\epsilon} \left(\frac{m_b}{\mu} \right)^{-4\epsilon} + 68.688 + \frac{1888}{81} i\pi \right) \times \frac{\alpha_s}{4\pi} \langle s\gamma | O_7 | b \rangle_{tree}$$

$$M_6 = \left(-\frac{4588}{243\epsilon} \left(\frac{m_b}{\mu} \right)^{-4\epsilon} - 25.956 + 12a(z) + 20b(z) - \frac{3200}{243} i\pi \right) \times \frac{\alpha_s}{4\pi} \langle s\gamma | O_7 | b \rangle_{tree}$$

where

$$\langle s\gamma | O_7 | b \rangle_{tree} = \frac{em_b}{8\pi^2} \bar{u}(p') \not{\epsilon} \not{q} R u(p). \quad (3.10)$$

These results are in a perfect agreement with those from [18].

The renormalization procedure is described in [18]. As we follow the same scheme we don't go into details. The final results for the renormalized matrix elements are given in Eq. (2.8).

4 Numerical results

In this section we will present the numerical results for the branching ratios of the decays $\bar{B} \rightarrow X_{s(d)}\gamma$. In our numerical analysis we will use the following values taken from [35]:

$$M_W = 80.425 \text{ GeV}, \quad M_Z = 91.1876 \text{ GeV}, \quad m_t^{pole} = 174.3 \pm 5.1 \text{ GeV}, \quad \alpha_{em} = 1/137.036. \quad (4.1)$$

For the semileptonic branching ratio we will use the averaged value $\mathcal{B}(B \rightarrow X_c \ell^+ \bar{\nu}_\ell)^{exp} = (10.90 \pm 0.23)\%$ from [36]. We use two-loop expression for the strong coupling constant $\alpha_s(\mu)$ with $\alpha_s(M_Z) = 0.1172 \pm 0.002$ [35]. For the Wolfenstein parameters of the CKM matrix we will use [37]

$$\rho = 0.162 \pm 0.046, \quad \eta = 0.347 \pm 0.027, \quad A = 0.83 \pm 0.02, \quad \lambda = 0.2240 \pm 0.0036 \quad (4.2)$$

As it was pointed out in [23], in the phenomenological analysis of $\bar{B} \rightarrow X_s\gamma$ an important issue is the definition of the mass of charm quark m_c in the matrix elements of the current-current operators O_1, O_2 . The pole mass have been used in earlier works (e.g. [17]). However, as it was argued in [23], the use of the running mass $m_c(\mu)$ with μ varying between m_c and m_b is more appropriate. We follow this choice using

$$\frac{m_c}{m_b} = 0.23 \pm 0.05 \quad (4.3)$$

in the matrix elements of the effective operators. Eq. (4.3) agrees with the numbers used in [28]. They are obtained using $m_c(m_c) = (1.25 \pm 0.10) \text{ GeV}$ and $m_b \equiv m_b^{1S} = (4.69 \pm 0.03) \text{ GeV}$ [39]. The latter value for m_b is used also anywhere else in the analysis.

Using these input parameters and the photon energy cutoff $E_0 = 1.6 \text{ GeV}$ ³ we obtain for the branching ratios:

$$\mathcal{B}(\bar{B} \rightarrow X_s\gamma) = \left(3.52_{-0.16}^{+0.03}(\mu_b)_{-0.07}^{+0.00}(\mu_W)_{-0.24}^{+0.22}(z)_{-0.02}^{+0.02}(\text{CKM}) \pm 0.16(\text{param}) \right) \times 10^{-4}, \quad (4.4)$$

$$\mathcal{B}(\bar{B} \rightarrow X_d\gamma) = \left(1.34_{-0.08}^{+0.01}(\mu_b)_{-0.03}^{+0.00}(\mu_W)_{-0.12}^{+0.13}(z)_{-0.17}^{+0.18}(\text{CKM}) \pm 0.07(\text{param}) \right) \times 10^{-5}. \quad (4.5)$$

³This corresponds to $\delta = 0.318$ for $m_b = 4.69 \text{ GeV}$.

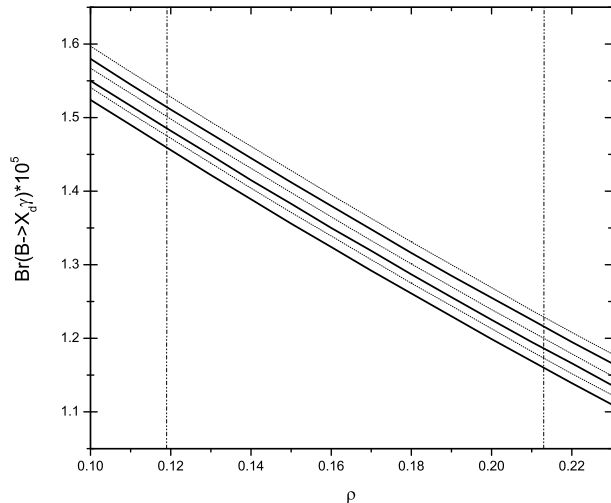


Figure 3: The dependence of $\mathcal{B}(\bar{B} \rightarrow X_d \gamma)$ on the CKM parameters ρ and η . Thick (thin) lines correspond to the branching ratio with matrix elements of QCD penguin operators included (excluded). The dependence on ρ is shown for three values of η : $\eta = 0.384$ (upper curves), $\eta = 0.356$ (middle curves) and $\eta = 0.328$ (lower curves). Vertical lines illustrate the experimental bounds on the parameter ρ .

The central values here correspond to the central values of the input parameters and $\mu_W = M_W$, $\mu_b = m_b$. We allow μ_b to vary between $m_b/2$ and $2m_b$ and the matching scale μ_W between M_W and m_t^{pole} . The last error sums up the uncertainties due to $\alpha_s(M_z)$, m_t^{pole} , $\mathcal{B}(\bar{B} \rightarrow X_c e \bar{\nu})^{exp}$ and the factor C (see Eq. (2.11)). The effect of the matrix elements of the QCD penguin operators calculated in this paper is -1.0% for $\bar{B} \rightarrow X_s \gamma$ and -1.1% for $\bar{B} \rightarrow X_d \gamma$. These corrections lead to a slight increase of the renormalization scale dependence. Combining all the uncertainties we get

$$\mathcal{B}(\bar{B} \rightarrow X_s \gamma) = (3.45 \pm 0.30) \times 10^{-4}, \quad (4.6)$$

$$\mathcal{B}(\bar{B} \rightarrow X_d \gamma) = (1.27 \pm 0.24) \times 10^{-5} \quad (4.7)$$

As we have mentioned in Section 2 in our numerical calculations we have neglected the long-distance contributions due to presence of intermediate u -quark loops. Due to CKM-suppression these corrections are negligible for $B \rightarrow X_s \gamma$ but can be sizeable for $B \rightarrow X_d \gamma$. This is another source of uncertainty of theoretical prediction for $B \rightarrow X_d \gamma$ that can be roughly estimated to be of order of 10% (see e.g. [24] for a more detailed discussion).

The results of our numerical analysis are somewhat lower than those from [23],[18]. Note that the central values in Eq. (4.5) will decrease by about 1% if we use the values from [23] for the input parameters. The numerical discrepancy is explained by the difference in methods used

in the analysis. The main difference is that in [23] the charm-quark and top-quark contributions are split and each of them is treated separately.

As we can see from Eq. (4.6) the uncertainty due to CKM parameters while being negligible for $\bar{B} \rightarrow X_s \gamma$ is still dominating for $\bar{B} \rightarrow X_d \gamma$. In Fig.3 we illustrate the dependence of $\mathcal{B}(\bar{B} \rightarrow X_d \gamma)$ on ρ and η .

To conclude, we have presented an independent calculation of the $\mathcal{O}(\alpha_s)$ corrections to the matrix elements of the QCD penguin operators O_3, \dots, O_6 . The effect of these corrections is about 1% decrease for the branching ratios. The updated predictions for the branching ratios are $(3.45 \pm 0.30) \times 10^{-4}$ for $\bar{B} \rightarrow X_s \gamma$ and $(1.27 \pm 0.24) \times 10^{-5}$ for $\bar{B} \rightarrow X_d \gamma$.

Acknowledgments

The work was partially supported by NFSAT-PH 095-02 (CRDF 12050) program. The work H. M. A. was partially supported by NATO Grant PST.CLG.978154.

Appendix A: Formulae for one-loop building blocks

In this appendix we will give the complete formulae of the one-loop building blocks for all different contributions described in section 3.1. All the calculations are done using the dimensional regularization in $d = 4 - 2\epsilon$ dimensions using the NDR scheme with fully anticommuting γ_5 . For both diagrams index β is to be contracted to the gluon propagator and α to the photon polarization vector. r and q denote the 4-momenta of the gluon and photon respectively.

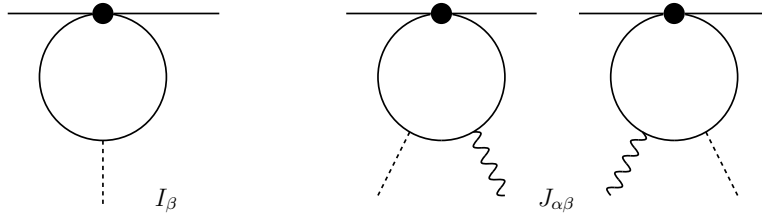


Figure 4: **One-loop building blocks used in our calculation.**

For type I insertion the contribution of the q -quark loop for the operators O_{iL} and O_{iR} ($q = s, b$; $i = 3, \dots, 6$) are respectively

$$I_{\beta(i)}^{q(I)}(L) \equiv -\bar{C}_i^I D_i^I(L) \frac{g_s}{4\pi^2} \Gamma(\epsilon) (1 - \epsilon) \mu^{2\epsilon} e^{\gamma_E \epsilon} e^{i\pi\epsilon} \int_0^1 \frac{dx [x(1-x)]^{1-\epsilon}}{\Delta^\epsilon} (r_\beta \not{r} - r^2 \gamma_\beta) L \frac{\lambda}{2}, \quad (\text{A.1})$$

$$I_{\beta(i)}^{q(I)}(R) \equiv -\bar{C}_i^I D_i^I(R) \frac{g_s}{4\pi^2} \Gamma(\epsilon) \epsilon \mu^{2\epsilon} e^{\gamma_E \epsilon} e^{i\pi\epsilon} \int_0^1 \frac{xdx [x(1-x)]^{-\epsilon}}{\Delta^\epsilon} m_q (\not{r} \gamma_\beta - \gamma_\beta \not{r}) R(q) \frac{\lambda}{2}, \quad (\text{A.2})$$

where $R(s) = L$, $R(b) = R$,

$$\Delta = r^2 - m_q^2/x(1-x) + i\delta. \quad (\text{A.3})$$

The operator-dependent color coefficients \bar{C}_i and Dirac algebra induced factors D_i are given by

$$\begin{aligned}\bar{C}_3^I &= \bar{C}_5^I = 1, & \bar{C}_4^I &= \bar{C}_6^I = -1/(2N_c); \\ D_3^I(L, R) &= D_4^I(L, R) = 1, \\ D_5^I(L) &= D_6^I(L) = 4(4 - \epsilon - \epsilon^2), & D_5^I(R) &= D_6^I(R) = 4(5 - 3\epsilon - \epsilon^2).\end{aligned}$$

For the type II insertions $I_\beta(R)$ apparently vanishes so we have ($q = u, d, s, c, b$; $i = 4, 6$)

$$\begin{aligned}I_{\beta(i)}^{q(II)} &\equiv I_{\beta(i)}^{q(II)}(L) = \\ &= -\bar{C}_i^{II} D_i^{II} \frac{g_s}{4\pi^2} \Gamma(\epsilon) \mu^{2\epsilon} e^{\gamma_E \epsilon} e^{i\pi\epsilon} \int_0^1 \frac{dx [x(1-x)]^{1-\epsilon}}{\Delta^\epsilon} (r_\beta \not{x} - r^2 \gamma_\beta) L \frac{\lambda}{2}\end{aligned}\quad (\text{A.4})$$

where

$$\begin{aligned}\bar{C}_3^{II} &= \bar{C}_5^{II} = 0, & \bar{C}_4^{II} &= \bar{C}_6^{II} = (1/2); \\ D_4^{II} &= 2, & D_6^{II} &= 4(5 - 3\epsilon).\end{aligned}$$

Similarly, for the type I contributions of operators O_{iL} and O_{iR} for the building block $J_{\alpha\beta}$ we have

$$\begin{aligned}J_{\alpha\beta(i)}^{q(I)}(L) &= A_i^I B_i^I(L) \frac{eg_s Q_q}{16\pi^2} \left[E(\alpha, \beta, r) \Delta i_5 + E(\alpha, \beta, q) \Delta i_6 - E(\beta, r, q) \frac{r_\alpha}{qr} \Delta i_{23} \right. \\ &\quad \left. - E(\alpha, r, q) \frac{r_\beta}{qr} \Delta i_{25} - E(\alpha, r, q) \frac{q_\beta}{qr} \Delta i_{26} \right] L \frac{\lambda}{2},\end{aligned}\quad (\text{A.5})$$

$$\begin{aligned}J_{\alpha\beta(i)}^{q(I)}(R) &= A_i^I m_q \epsilon \frac{eg_s Q_q}{16\pi^2} \Gamma(\epsilon) \int_S dx dy C^{-1-\epsilon} [8(g_{\alpha\beta}(qr) - r_\alpha q_\beta) \\ &\quad \times (dxy B_i^{1I}(R) - 2B_i^{2I}(R)) + 2(2 + \epsilon) B_i^{3I}(R) (\not{x} \gamma_\beta \gamma_\alpha \not{x} + \not{x} \gamma_\alpha \gamma_\beta \not{x})] L \frac{\lambda}{2}\end{aligned}\quad (\text{A.6})$$

where

$$E(\alpha, \beta, r) = \frac{1}{2} (\gamma_\alpha \gamma_\beta \not{x} - \not{x} \gamma_\beta \gamma_\alpha). \quad (\text{A.7})$$

The operator-dependent color coefficients A_i and Dirac algebra induced factors B_i are given by

$$\begin{aligned}A_3^I &= A_5^I = 1, & A_4^I &= A_6^I = -1/(2N_c); \\ B_3^{jI}(L, R) &= B_4^{jI}(L, R) = 1, & j &= 1, 2, 3, \\ B_5^I(L) &= B_6^I(L) = 4(4 - 5\epsilon - \epsilon^2), & B_5^{1I}(R) &= B_6^{1I}(R) = 4(1 + \epsilon - \epsilon^2), \\ B_5^{2I}(R) &= B_6^{2I}(R) = 4(1 - 3\epsilon - 3\epsilon^2), & B_5^{3I}(R) &= B_6^{3I}(R) = 4(1 - 7\epsilon - \epsilon^2).\end{aligned}\quad (\text{A.8})$$

Finally the quantities Δ_i are defined as in [17]

$$\begin{aligned}\Delta i_{23} &= -\Delta i_{26} = 8(qr) \int_S dx dy [xy \epsilon (1 + \epsilon) \Gamma(\epsilon) \exp(\gamma_E \epsilon) \mu^{2\epsilon} C^{-1-\epsilon}], \\ \Delta i_{25} &= -8(qr) \int_S dx dy [x(1-x) \epsilon (1 + \epsilon) \Gamma(\epsilon) \exp(\gamma_E \epsilon) \mu^{2\epsilon} C^{-1-\epsilon}], \\ \Delta i_5 &= \Delta i_{23}, & \Delta i_6 &= \frac{r^2}{(qr)} \Delta i_{25} + \Delta i_{26},\end{aligned}\quad (\text{A.9})$$

where C is given by

$$C = m_q^2 - 2xy(qr) - x(1-x)r^2 - i\delta$$

In the case of type II contributions we have

$$\begin{aligned} J_{\alpha\beta(i)}^{q(II)}(L) &= A_i^{II} B_i^{II}(L) \frac{eg_s Q_q}{16\pi^2} \left[E(\alpha, \beta, r) \Delta i_5 + E(\alpha, \beta, q) \Delta i_6 - E(\beta, r, q) \frac{r_\alpha}{qr} \Delta i_{23} \right. \\ &\quad \left. - E(\alpha, r, q) \frac{r_\beta}{qr} \Delta i_{25} - E(\alpha, r, q) \frac{q_\beta}{qr} \Delta i_{26} \right] L \frac{\lambda}{2}, \end{aligned} \quad (\text{A.10})$$

where

$$\begin{aligned} B_3^{II} &= B_4^{II} = B_5^{II} = 0, \quad B_6^{II} = -24/(6-d) \\ A_6^{II} &= 1/2. \end{aligned}$$

Appendix B: Formulae for bremsstrahlung corrections

Here we list the formulae for the bremsstrahlung coefficients f_{ij}^{ab} ^{4 5}:

$$\begin{aligned} f_{22}^{cc} &= \frac{16z}{27} \left[\delta \int_0^{(1-\delta)/z} dt (1-zt) \left| \frac{G(t)}{t} + \frac{1}{2} \right|^2 + \int_{(1-\delta)/z}^{1/z} dt (1-zt)^2 \left| \frac{G(t)}{t} + \frac{1}{2} \right|^2 \right], \\ f_{27}^{cc} &= -\frac{4z^2}{9} \left[\delta \int_0^{(1-\delta)/z} dt \left(G(t) + \frac{t}{2} \right) + \int_{(1-\delta)/z}^{1/z} dt (1-zt) \left(G(t) + \frac{t}{2} \right) \right], \\ f_{78}^{cc} &= \frac{4}{9} \left[\text{Li}_2(1-\delta) - \frac{\pi^2}{6} - \delta \ln \delta + \frac{9}{4}\delta - \frac{1}{4}\delta^2 + \frac{1}{12}\delta^3 \right], \\ f_{77}^{cc} &= \frac{1}{3} \left[10\delta + \delta^2 - \frac{2\delta^3}{3} + \delta(\delta-4) \ln \delta \right], \\ f_{88}^{cc} &= \frac{1}{27} \left[-2 \ln \frac{m_b}{m_s} (\delta^2 + 2\delta + 4 \ln(1-\delta)) \right. \\ &\quad \left. + 4\text{Li}_2(1-\delta) - \frac{2\pi^2}{3} - \delta(2+\delta) \ln \delta + 8 \ln(1-\delta) - \frac{2}{3}\delta^3 + 3\delta^2 + 7\delta \right], \\ f_{22}^{uc} &= \frac{8z}{27} \left[\delta \int_0^{(1-\delta)/z} dt (1-zt) \left(\frac{G^*(t)}{t} + \frac{1}{2} \right) + \int_{(1-\delta)/z}^{1/z} dt (1-zt)^2 \left(\frac{G^*(t)}{t} + \frac{1}{2} \right) \right], \\ f_{27}^{uc} &= -\frac{1}{27} \delta (3 - 3\delta + \delta^2) \\ f_{22}^{uu} &= -\frac{2}{81} \delta (\delta^2 - 3), \end{aligned} \quad (\text{B.1})$$

⁴Note that our definitions of quantities f_{ij}^{cc} slightly differ from the standard definitions of f_{ij} (see e.g.[16])

⁵The formula for the coefficient f_{88} is the only place where the mass of the final state quark has to be retained due to logarithmic divergence. This collinear divergences can be resummed to all orders in perturbation theory [38]. However, for realistic values of m_s and m_d the contribution of f_{88} is under 1%, so we will ignore this issue using $m_b/m_s = 50$ and $m_b/m_d = 1000$ in our analysis.

where the function $G(t)$ is defined in Eq. (40) of [16]. The other coefficients can be expressed in terms of those defined above:

$$\begin{aligned}
f_{11}^{cc} &= \frac{1}{36}f_{22}^{cc}, & f_{12}^{cc} &= -\frac{1}{6}f_{22}^{cc}, & f_{28}^{cc} &= -\frac{1}{3}f_{27}^{cc}, & f_{17}^{cc} &= -\frac{1}{6}f_{27}^{cc}, & f_{18}^{cc} &= -\frac{1}{6}f_{28}^{cc}, \\
f_{11}^{uc} &= \frac{1}{36}f_{22}^{uc}, & f_{12}^{uc} &= -\frac{1}{3}f_{22}^{uc}, & f_{28}^{uc} &= -\frac{1}{3}f_{27}^{uc}, & f_{17}^{uc} &= -\frac{1}{6}f_{28}^{uc}, & f_{18}^{uc} &= -\frac{1}{6}f_{27}^{uc}, \\
f_{11}^{uu} &= \frac{1}{36}f_{22}^{uu}, & f_{12}^{uu} &= -\frac{1}{6}f_{22}^{uu},
\end{aligned}
\tag{B.2}$$

Finally we have

$$f_{ji} = f_{ij}^* \tag{B.3}$$

for the quantities defined in Eqs. (B.1), (B.2). In the bremsstrahlung corrections we have used the same value $m_c/m_b = 0.23 \pm 0.05$ as in Eq. (4.3).

References

- [1] M. S. Alam *et al.* [CLEO Collaboration], Phys. Rev. Lett. **74**, 2885 (1995).
- [2] R. Barate *et al.* [ALEPH Collaboration], Phys. Lett. B **429**, 169 (1998).
- [3] B. Aubert *et al.* [BABAR Collaboration], hep-ex/0207074.
- [4] B. Aubert *et al.* [BaBar Collaboration], hep-ex/0207076.
- [5] K. Abe *et al.* [Belle Collaboration], Phys. Lett. B **511**, 151 (2001), hep-ex/0103042.
- [6] S. Chen *et al.* [CLEO Collaboration], Phys. Rev. Lett. **87**, 251807 (2001), hep-ex/0108032.
- [7] S. Stone, hep-ph/0310153.
- [8] B. Aubert *et al.* [BABAR Collaboration], hep-ex/0306038.
- [9] A. J. Buras, M. Misiak, M. Munz and S. Pokorski, Nucl. Phys. B **424** (1994) 374, hep-ph/9311345.
- [10] M. Misiak and M. Munz, Phys. Lett. B **344**, 308 (1995), hep-ph/9409454.
- [11] K. Adel and Y. P. Yao, Phys. Rev. D **49**, 4945 (1994), hep-ph/9308349.
- [12] C. Greub and T. Hurth, Phys. Rev. D **56**, 2934 (1997), hep-ph/9703349.
- [13] A. J. Buras, A. Kwiatkowski and N. Pott, Nucl. Phys. B **517**, 353 (1998), hep-ph/9710336.
- [14] A. Ali and C. Greub, Phys. Lett. B **361**, 146 (1995), hep-ph/9506374.

- [15] N. Pott, Phys. Rev. D **54**, 938 (1996), hep-ph/9512252.
- [16] K. G. Chetyrkin, M. Misiak and M. Munz, Phys. Lett. B **400** (1997) 206, hep-ph/9612313.
- [17] C. Greub, T. Hurth and D. Wyler, Phys. Rev. D **54** (1996) 3350, hep-ph/9603404.
- [18] A. J. Buras, A. Czarnecki, M. Misiak and J. Urban, Nucl. Phys. B **631** (2002) 219, hep-ph/0203135.
- [19] A. F. Falk, M. Luke and M. J. Savage, Phys. Rev. D **49**, 3367 (1994), hep-ph/9308288.
- [20] M. B. Voloshin, Phys. Lett. B **397**, 275 (1997), hep-ph/9612483.
- [21] G. Buchalla, G. Isidori and S. J. Rey, Nucl. Phys. B **511**, 594 (1998), hep-ph/9705253.
- [22] P. Gambino and U. Haisch, JHEP **0009**, 001 (2000), hep-ph/0007259; JHEP **0110**, 020 (2001), hep-ph/0109058.
- [23] P. Gambino and M. Misiak, Nucl. Phys. B **611** (2001) 338, hep-ph/0104034.
- [24] A. Ali, H. Asatrian and C. Greub, Phys. Lett. B **429** (1998) 87, hep-ph/9803314.
- [25] H. H. Asatrian and H. M. Asatrian, Phys. Lett. B **460**, 148 (1999), hep-ph/9906221.
- [26] H. H. Asatryan, H. M. Asatrian, G. K. Yeghiyan and G. K. Savvidy, Int. J. Mod. Phys. A **16**, 3805 (2001), hep-ph/0012085.
- [27] A. J. Buras, A. Czarnecki, M. Misiak and J. Urban, Nucl. Phys. B **611** (2001) 488, hep-ph/0105160.
- [28] T. Hurth, E. Lunghi and W. Porod, hep-ph/0312260.
- [29] A. H. Hoang, Z. Ligeti and A. V. Manohar, Phys. Rev. D **59**, 074017 (1999), hep-ph/9811239; Phys. Rev. Lett. **82** (1999) 277, hep-ph/9809423.
- [30] G. Ricciardi, Phys. Lett. B **355**, 313 (1995) [arXiv:hep-ph/9502286].
- [31] N. G. Deshpande, X. G. He and J. Trampetic, Phys. Lett. B **367**, 362 (1996).
- [32] C. Greub and P. Liniger, Phys. Rev. D **63** (2001) 054025; Phys. Lett. B **494** (2000) 237.
- [33] H. H. Asatrian, H. M. Asatrian, C. Greub and M. Walker, Phys. Lett. B **507** (2001) 162; Phys. Rev. D **65** (2002) 074004.
- [34] A. L. Kagan and M. Neubert, Eur. Phys. J. C **7**, 5 (1999), hep-ph/9805303.
- [35] K. Hagiwara *et al.* [Particle Data Group Collaboration], Phys. Rev. D **66**, 010001 (2002). See also the web site: <http://pdg.lbl.gov/>.

- [36] See <http://www.slac.stanford.edu/xorg/hfag/>.
- [37] M. Battaglia *et al.*, hep-ph/0304132.
- [38] A. Kapustin, Z. Ligeti and H. D. Politzer, Phys. Lett. B **357** (1995) 653, hep-ph/9507248.
- [39] A. H. Hoang, hep-ph/0008102.